

RESEARCH

Open Access



# Oncogenic role of fumarate hydratase in breast cancer: metabolic reprogramming and mechanistic insights

Shyng-Shiou F. Yuan<sup>1,2,3,4,5,6\*</sup>, Anupama Vadhan<sup>1,16†</sup>, Hieu D. H. Nguyen<sup>7</sup>, Pang-Yu Chen<sup>1</sup>, Chih-Huang Tseng<sup>7,8</sup>, Ching-Hu Wu<sup>3</sup>, Yu-Chieh Chen<sup>3</sup>, Yi-Chia Wu<sup>9,10,11</sup>, Stephen Chu-Sung Hu<sup>12,13</sup>, Steven Lo<sup>14</sup>, Ming-Feng Hou<sup>11,15</sup> and Yen-Yun Wang<sup>4,5,7\*</sup>

## Abstract

Breast cancer remains the most prevalent malignancy among women globally, with its complexity linked to genetic variations and metabolic alterations within tumor cells. This study investigates the role of fumarate hydratase (FH), a key enzyme in the tricarboxylic acid (TCA) cycle, in breast cancer progression. Our findings reveal that FH mRNA and protein levels are significantly upregulated in breast cancer tissues and correlate with poor patient prognosis and aggressive tumor characteristics. Using in vitro and in vivo models, we demonstrate that FH overexpression enhances breast cancer cell proliferation, migration, and invasion through metabolic reprogramming and by increasing reactive oxygen species (ROS) production. Furthermore, we identify matrix metalloproteinase 1 (MMP1) as a downstream effector of FH, linked to p21 downregulation, elucidating a novel regulatory pathway influencing tumor behavior. Interestingly, unlike its tumor-suppressing role in other cancer types, this study highlights FH's oncogenic potential in breast cancer. Our results suggest that FH enhances cancer cell viability and aggressiveness via both catalytic and non-catalytic mechanisms. This work not only underscores the metabolic adaptations of breast cancer cells but also proposes FH as a potential biomarker and therapeutic target for breast cancer management.

## Introduction

Breast cancer represents the most commonly diagnosed malignancy among women globally, with a significant upward trend in incidence rates [1]. The progression of the disease, available therapeutic options, and the response to treatment are influenced by genetic variations within the breast epithelium and the surrounding microenvironment [2]. Although numerous genes and proteins have been scrutinized in the context of breast

cancer, metabolic reprogramming has emerged as a pivotal factor in cancer advancement [3, 4]. Consequently, metabolomics-based biomarkers and targeted therapies could offer promising alternatives for patients who exhibit resistance to existing treatments.

Metabolic reprogramming is recognized as a hallmark of cancer cells, facilitating sustained growth and proliferation [5, 6]. Otto Warburg's seminal discovery in 1924, now termed the "Warburg effect," demonstrated that cancer cells preferentially utilize anaerobic glycolysis for ATP generation, even in oxygen-rich environments, diverging from normal cellular metabolism [7]. While glycolysis was initially considered the primary energy source for cancer cells as opposed to mitochondrial respiration in healthy cells [8], recent studies underscore the

<sup>†</sup>Shyng-Shiou F. Yuan and Anupama Vadhan are co-first author.

\*Correspondence:  
Shyng-Shiou F. Yuan  
yuanssf@kmu.edu.tw  
Yen-Yun Wang  
wyy@kmu.edu.tw

Full list of author information is available at the end of the article



importance of mitochondrial dysfunction in driving cancer cell proliferation and progression [9, 10].

The tricarboxylic acid (TCA) cycle, also referred to as the Krebs cycle, takes place in the mitochondria and is integral to the metabolism of carbohydrates, lipids, and amino acids [11, 12]. This pathway enables aerobic organisms to oxidize biological substrates, thereby generating energy while maintaining macromolecular synthesis and redox balance within cells [13]. In normal tissues, glucose metabolism occurs via conversion to pyruvate in the cytosol, which is subsequently oxidized in aerobic conditions by pyruvate dehydrogenase and various TCA cycle enzymes. Recently, the non-metabolic roles of TCA cycle enzymes have garnered heightened attention in cancer research [14–16].

Fumarate hydratase (FH), an enzyme within the TCA cycle, catalyzes the reversible hydration of fumarate to malate, exhibiting dual localization and functionality within both mitochondrial and cytosolic/nuclear compartments of eukaryotic cells [17]. In human cells, FH plays a role in DNA repair through the non-homologous end joining (NHEJ) pathway [17], and has been implicated as a tumor suppressor [18, 19]. Mutations in the FH gene are associated with a predisposition to multiple cutaneous and uterine leiomyomas (MCUL) and hereditary leiomyomatosis and renal cell carcinoma (HLRCC). In contrast, recessive mutations can lead to severe outcomes, including early mortality and acute encephalopathy [20]. In renal cancer models deficient in FH, metabolic shifts towards aerobic glycolysis occur, with both glycolytic and tumorigenic phenotypes reverting upon restoration of FH activity [21]. Furthermore, FH has demonstrated tumor suppressive properties in lung and endometrial cancers [22, 23].

Currently, the specific role of FH in breast cancer remains poorly defined. Notably, mutations in FH are infrequently observed in breast carcinoma [24]. While DNA methylation typically affects the promoter regions of tumor suppressor genes in various cancers, such modifications are absent in the FH promoter region within breast carcinoma [25]. Investigations have highlighted that Rutaecarpine, an experimental anti-cancer agent, promotes differentiation of triple-negative breast cancer cells and inhibits fumarate hydratase activity [26], while mitochondrial long non-coding RNA GAS5 has been identified as a tumor suppressor that disrupts the metabolic functions of FH [27].

In this study, we aim to investigate the role of FH in breast cancer by starting with its expression in breast cancer tissues and its correlation with established prognostic markers using online databases including Oncomine and Km.plot, followed by functional investigation into the implications of FH in breast cancer pathophysiology.

## Methods

### Patient samples

Breast cancer tissues were collected from patients who underwent surgical treatment at the Department of Surgery, Kaohsiung Medical University Hospital, Taiwan (Approval numbers: KMUHIRB-F(I)–20,180,112, KMUHIRB-E(I)–20,180,136, KMUHIRB-E(I)–20,200,299). Overall survival (OS) was defined as the time from diagnosis to death, while disease-free survival (DFS) was measured from diagnosis or the start of treatment to the first recurrence.

### Immunohistochemistry

Tissues for the immunohistochemistry study were sourced from formalin-fixed, paraffin-embedded blocks. Immunohistochemical (IHC) staining for fumarate hydratase (FH) was conducted using the Bond-Max system (Leica Microsystems, Wetzlar, Germany). FH expression in the breast cancer specimens was evaluated with the TissueFAXS microscopy system and HistQuest software (TissueGnostics, Vienna, Austria). IHC scores were assigned based on FH staining intensity in cancer cells: 0, 1+, 2+, or 3+, with 0/1+ indicating low expression and 2+/3+ indicating high expression.

### Cell culture

The human breast cancer cell lines MDA-MB-231, BT-20, HS578 T, MCF-7, BT-474, ZR75-1, T47D, and the mouse breast carcinoma cell line 4T1 were obtained from the Bioresource Collection and Research Center (BCRC, Hsinchu, Taiwan). The BT-549 human breast cancer cell line was sourced from ATCC. MDA-MB-231, HS578 T, MCF-7, T47D, ZR75-1, and BT-474 cells were maintained in DMEM medium. BT-20 cells were maintained in EMEM medium, whereas BT-549 and 4T1 cells were maintained in RPMI-1640 medium. All culture media were supplemented with 10% fetal bovine serum, 1% penicillin G, and streptomycin.

### Lentiviral infection for FH knockdown and overexpression

To silence fumarate hydratase in breast cancer cells, we used lentiviruses carrying the pLKO.1\_puro lentiviral vector expressing shRNA targeting human fumarate hydratase (four clones: TRCN0000052466, TRCN0000310398, TRCN0000052465, TRCN0000299140). Each clone had specific target sequences and oligo sequences. A lentiviral vector expressing shRNA targeting firefly luciferase, which does not match any human sequence, served as a negative control (National RNAi Core Facility, Academia Sinica, Taiwan).

For overexpression, we used lentiviral particles containing the pReceiver Lv105 vector expressing the human

fumarate hydratase gene, obtained from Genecopoeia (Rockville, MD). Lentiviral particles with an empty pReceiver Lv105 vector served as a negative control. Lentiviral infection was carried out by adding virus solution to culture media supplemented with 8 µg/mL polybrene. For selection, 2 µg/mL puromycin was added 24 h post-infection, and surviving cells were maintained in 2 µg/mL puromycin throughout the experiment.

#### XTT colorimetric assay

Cell proliferation rates were assessed using the XTT colorimetric assay, which involves 2,3-Bis(2-methoxy-4-nitro-5-sulfophenyl)-2H-tetrazolium-5-carboxanilide (XTT) (Roche Molecular Biochemicals, Germany). The procedure followed was based on previously published reports [28, 29]. Cell viability was assessed at two time points, 24 and 48 h.

#### Cell cycle analysis

Cells were trypsinized, then fixed in 1 mL of 70% ethanol overnight at 4 °C. Following this, they were centrifuged at 1500 g for 5 min and resuspended in 1 mL of phosphate-buffered saline (PBS) containing 50 µg/mL RNase and 50 µg/mL propidium iodide (Sigma Chemical Co., St. Louis, MO). The stained cells were analyzed using flow cytometry (BD, Becton, Dickinson & Co).

#### Transwell migration and invasion assays

The cell migration assay was conducted using 24-well plates with Transwell membrane filter inserts (6.5 mm diameter, 8 µm pore size; Corning Costar Corp., Cambridge, MA, USA). Breast cancer cells, subjected to fumarate hydratase overexpression or knockdown, were seeded in serum-free medium in the upper chamber of the Transwell filters. The lower chamber contained serum-supplemented medium. Cells were incubated for 24 h at 37 °C, then fixed with 4% formaldehyde and stained with crystal violet. Non-migrating cells were removed from the filter's upper surface, while migrated cells were imaged using an Olympus SZX10 microscope and analyzed with ImageJ software.

For invasion assays, BioCoat Matrigel invasion chambers (Corning, BioCoat™) were rehydrated following the manufacturer's instructions, with subsequent steps mirroring those of the migration assay.

#### Western blot analysis

Western blotting was employed to evaluate knockdown efficiency post-lentivirus infection and to examine the expression of various proteins, following the methodology described in a prior study (23). After protein transfer, the polyvinylidene fluoride (PVDF) membrane was incubated overnight with primary antibodies. Protein

bands were visualized using an enhanced chemiluminescence reagent (Perkin Elmer, American Fork, UT, USA) and Image Lab software (BIO-RAD). MMP1 inhibitor GM6001 (Ilomastat, HY-15768) and p21 inhibitor UC2288 (532,813) were procured from Sigma and used to treat breast cancer cells for 6 h and 48 h, respectively, before collection for Western blot analysis.

#### Mito stress test

The Mito Stress Test was performed using the Agilent Seahorse XFe/XF Analyzer along with the Agilent Seahorse XF Cell Mito Stress Test Kit. To measure multiple statuses of OCR in mitochondria, an Agilent Seahorse XFe24 Analyzer (Agilent Technologies, Santa Clara, CA, USA) was used in accordance with the procedures from the manufacturer and our previous report [28]. The mitochondrial modulators were obtained from Seahorse XF Cell Mito Stress Test Kit (Agilent Technologies, Santa Clara, CA, USA) and injected sequentially for specific measurements as follows: first, 1 µM oligomycin was injected to measure ATP production; second, 0.5 µM carbonyl cyanide 4-(trifluoromethoxy)phenylhydrazone (FCCP) was injected to measure maximal respiration; finally, 0.5 µM rotenone and 0.5 µM antimycin A were injected to measure spare respiratory capacity. The OCR and ECAR values were normalized by the final cell numbers.

#### ECAR and OCR analysis by CLARIOstar

For extracellular acidification rate (ECAR) measurement, FH-overexpressing breast cancer cells were seeded in 96-well plates at a density of  $8 \times 10^4$  cells per well in 200 µL of medium. After 24 h, the plate was placed in a CO<sub>2</sub>-free incubator for 3 h to deplete CO<sub>2</sub>. The medium was then replaced with 150 µL of respiration buffer and 10 µL of glycolysis reagent in each well. ECAR was measured using a CLARIOstar plate reader (BMG Labtech) over a period of 200 min.

For oxygen consumption rate (OCR) analysis, FH-overexpressing breast cancer cells were also seeded in 96-well plates at a density of  $8 \times 10^4$  cells per well in 200 µL of medium. After 24 h, the medium was refreshed with new medium containing the O<sub>2</sub> reagent. Each well was immediately covered with pre-warmed mineral oil to minimize evaporation. OCR was then measured using the CLARIOstar (BMG Labtech) for 120 min [28].

#### Measurement of cellular reactive oxygen species (ROS)

Cellular ROS were detected using flow cytometry. Cells were incubated with 2',7'-dichlorodihydrofluorescein diacetate (DCFH-DA, 10 µM, Sigma-Aldrich) for 30 min at 37 °C, after which the cells were washed, suspended in ice-cold PBS, and analyzed for fluorescence intensity

using a 485 nm excitation beam (BD, Becton, Dickinson & Co). Flow Jo 7.6 was utilized to quantify the mean fluorescence intensity.

### Animal study

All animal experimentation was conducted in compliance with the Institutional Animal Care and Utilization Committee of Kaohsiung Medical University, Kaohsiung, Taiwan (IACUC number: 109046). The number of animals used was thoughtfully designed and minimized to adhere to the principles of the three Rs (Replacement, Reduction, and Refinement). In the syngeneic orthotopic mouse model,  $1 \times 10^6$  Luc-4 T1 mouse breast cancer cells, either with or without fumarate hydratase (FH) knockdown, were injected into the fourth mammary fat pads of female BALB/c mice, aged six to eight weeks (Lasco, Taiwan). The bioluminescent signals from Luc-4 T1 cells were monitored using an in vivo imaging system (IVIS) over a period of 7 weeks, after which the mice were sacrificed for hematoxylin–eosin staining and immunohistochemical (IHC) analysis.

### Statistical analysis

Statistical analyses were conducted using the SPSS version 14.0 statistical software package for PC (SPSS, Inc., Chicago, IL). The association between fumarate hydratase expression and various variables—such as stage, grade, age, tumor size, and lymph node metastasis—was assessed using Chi-square tests. Kaplan–Meier estimates were employed to generate survival curves, with differences between curves evaluated using the log-rank test. Both univariate and multivariable Cox regression models were utilized to examine the relationships between clinicopathological characteristics and overall survival. To analyze the data in all other experiments, student t-test was used. A statistical significance threshold was set at  $p < 0.05$ .

## Results

### FH mRNA and protein upregulation in breast cancer tissue correlates with malignant behavior and poor prognosis

Fumarate hydratase (FH) expression in breast cancer was initially evaluated using online datasets from Oncomine, Km.plot, Human Protein Atlas, and UALCAN [30–33]. Analysis revealed that FH mRNA levels were significantly

higher in breast cancer tissues compared to normal tissues (Fig. 1A & B). Furthermore, elevated FH expression was associated with poor survival outcomes for patients (Fig. 1C & D). To assess FH protein levels, immunohistochemistry (IHC) was performed on breast cancer tissues (Fig. 1E), correlating FH expression with various clinicopathological characteristics. Survival analysis using the log-rank test indicated that high FH expression was linked to shorter disease-free survival (DFS,  $p = 0.022$ ) and overall survival (OS,  $p = 0.030$ ) compared to low FH expression (Fig. 1F). Additional analysis showed that high FH expression in breast cancer tissues positively correlated with larger tumor size (T status,  $p = 0.007$ ) and lymph node metastasis (N status,  $p = 0.011$ ) (Table 1). Univariate and multivariate Cox regression analyses demonstrated that FH was a significant predictor of patient survival (HR = 6.54 for univariate and HR = 4.85 for multivariate analyses, respectively, as shown in Tables 2 and 3).

Using UALCAN, we further analyzed FH expression based on cancer stage, breast cancer subclass, nodal metastasis, and TP53 status. This analysis showed elevated FH expression in breast cancer adenocarcinoma (BRCA), independent of cancer stage, subclass, nodal metastasis, and TP53 mutation status (Supplementary Fig. S1).

### Upregulated FH expression enhances cell viability, migration, and invasion

FH protein levels were assessed across eight breast cancer cell lines, comprising four luminal and four basal types (Supplementary Fig. S2 A). MCF-7 luminal and MDA-MB-231 basal-like cells were selected for further investigation based on their FH expression profiles. FH overexpression led to increased cell proliferation in both MCF-7 and MDA-MB-231 cells (Fig. 2A). For FH knockdown, four shRNA clones were evaluated, and shRNA1 (KD1) and shRNA2 (KD2) were selected for their superior knockdown efficiency (Supplementary Fig. S2B). Cells with FH knockdown exhibited reduced proliferation compared to the control group (Shluc) (Fig. 2B).

Cell cycle distribution analysis revealed that FH knockdown cells were enriched in the G0/G1 phase (Supplementary Fig. S2 C) and displayed increased p21 protein expression (Supplementary Fig. S2D). Further analysis

(See figure on next page.)

**Fig. 1** Breast cancer tissues showed high expression of FH mRNA and protein, which were associated with poor survival in breast cancer patients. **A** & **B** FH mRNA expression in normal and tumor tissues from online datasets Oncomine and TCGA. **C** & **D** Kaplan–Meier OS analysis, according to FH mRNA expression using publicly available breast cancer online datasets Human Protein Atlas and Km.plot. **E** Protein expression of FH in normal breast and breast cancer tissues, determined by immunohistochemistry of patients' samples obtained from KMUH, Taiwan. **F** Kaplan–Meier survival analysis of the association of FH expression in breast cancer tissues with disease-free survival and overall survival

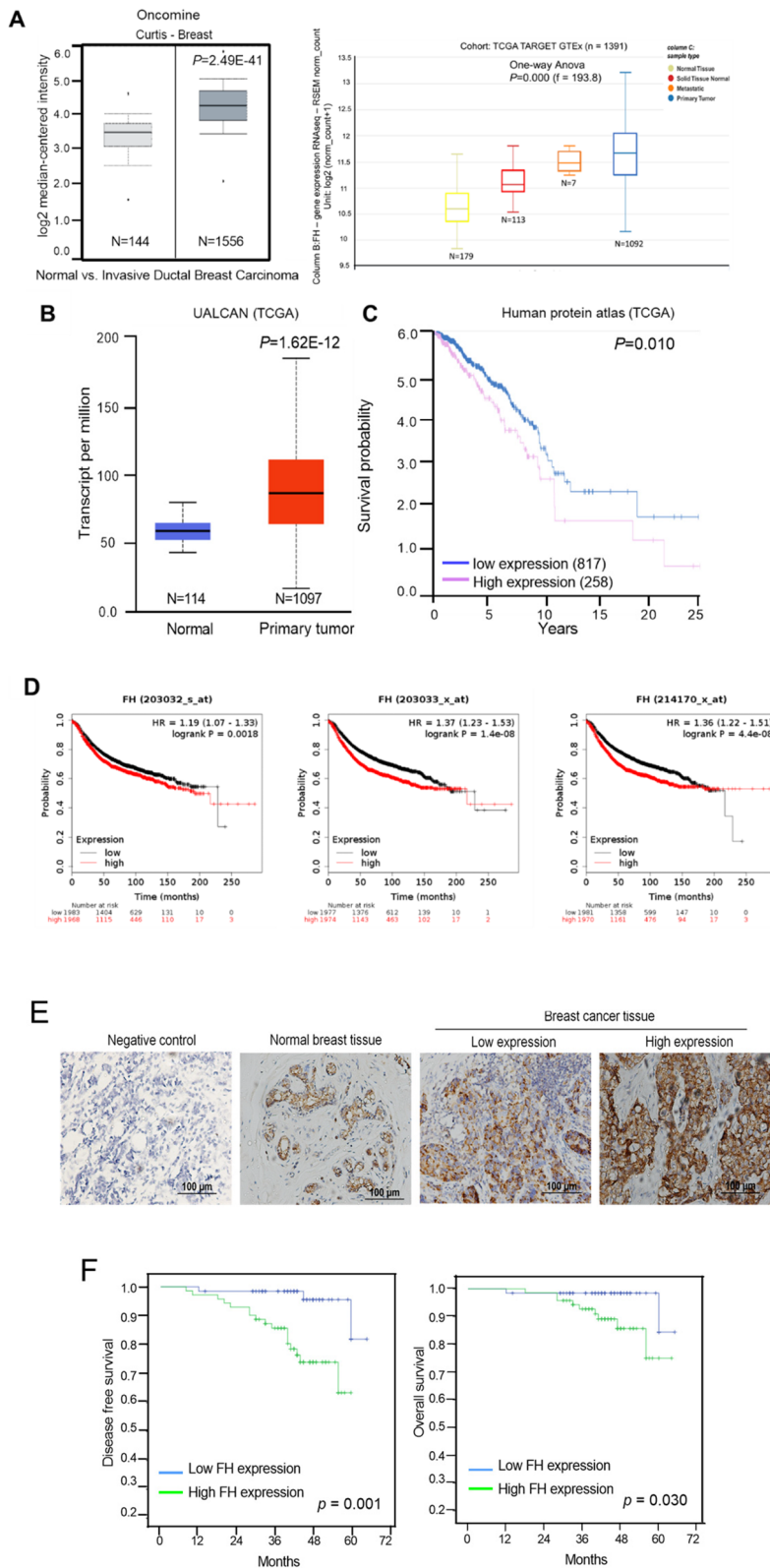


**Fig. 1** (See legend on previous page.)

**Table 1** Correlation of FH expression with clinicopathological characteristics in breast cancer

Variables	Categories	FH				p-Value*
		Low		High		
		N	%	N	%	
Age (y)	≤50	30	46.9	36	50.7	0.657
	>50	34	53.1	35	49.3	
Grade	I/II	51	79.7	48	67.6	0.113
	III	13	20.3	23	32.4	
T status	T1	41	64.1	29	40.8	0.007*
	T2-T4	23	35.9	42	59.2	
N status	N0	41	64.1	30	42.3	0.011*
	N1-3	23	35.9	41	57.7	
M status	M0	62	96.9	67	94.4	0.683
	M1	2	3.1	4	5.6	
BMI (kg/m <sup>2</sup> )	< 24	45	70.3	39	54.9	0.066
	≥24	19	29.7	32	45.1	
ER	Negative	19	29.7	27	38	0.307
	Positive	45	70.3	44	62	
PR	Negative	28	43.8	32	45.1	0.877
	Positive	36	56.2	39	54.9	
Her2/Neu	Negative	32	50	42	59.2	0.286
	Positive	32	50	29	40.8	
Chemotherapy	No	7	10.9	5	7	0.427
	Yes	57	89.1	66	93	
Radiotherapy	No	31	48.4	24	33.8	0.084
	Yes	33	51.6	47	66.2	
Hormone therapy	No	21	32.8	28	39.4	0.424
	Yes	43	67.2	43	60.6	

\*The p-Value was calculated by the chi-square test

confirmed enhanced migration and invasion abilities in FH-overexpressing breast cancer cells (Fig. 2C), while FH knockdown resulted in decreased migration and invasion capabilities (Fig. 2D).

#### Increased oxygen consumption rate in FH-overexpressing cells

To assess the role of FH in energy production, we measured the extracellular acidification rate (ECAR) as an indicator of glycolysis, and the oxygen consumption rate (OCR) as an indicator of respiration rate, in both FH-overexpressing and FH-knockdown cells. FH overexpression resulted in elevated OCR, but not ECAR, in both MDA-MB-231 and MCF-7 cells (Fig. 3 A & B; Supplementary Fig. S3 A-D). Conversely, FH knockdown led to decreased OCR, but not ECAR, levels (Fig. 3C & D). Given that reactive oxygen species (ROS) are produced as byproducts during respiration and may affect cancer cell behavior (34), we assessed ROS levels in FH-overexpressing and FH-knockdown cells. Results demonstrated that ROS production increased in FH-overexpressing cells

(Fig. 3E) but decreased in FH-knockdown cells (Fig. 3F). When the cells were treated with ROS scavengers, N-acetylcysteine (NAC) and ascorbic acid, the proliferation induced by FH overexpression was diminished (Fig. 3G; Supplementary Fig. S3E).

#### FH overexpression-induced breast cancer cell proliferation reduced by mitochondrial complex inhibitors

Mitochondrial electron transport chain (ETC) complexes I and III are principal sources of reactive oxygen species (ROS) generated during cellular respiration [34]. To determine if ROS produced by complex III contributed to the enhancement of proliferation and migration in FH-overexpressing cells, we assessed cell viability following treatment with antimycin (a complex III inhibitor). The proliferation of FH-overexpressing (FH-OE) cells was significantly diminished compared to the control group after antimycin treatment (Fig. 4A), indicating that FH overexpression increases the oxygen consumption rate (OCR) and promotes cell proliferation via ROS production from complex III. Additionally, migration

**Table 2** Univariate and multivariable analysis of disease-free survival for breast cancer patients

Variables	Categories	Univariate		Multivariable	
		HR (95%CI)	p-Value	HR (95%CI)	p-Value
Age (y)	>50	1.47 (0.60–3.60)	0.403		
	≤50	1			
Grade	III	1.54 (0.61–3.88)	0.359		
	I/II	1			
T status	T2-T4	1.51 (0.62–3.68)	0.365		
	T1	1			
N status	N1-3	1.62 (0.66–3.97)	0.292		
	N0	1			
BMI (kg/m <sup>2</sup> )	≥24	2.75 (1.12–6.76)	0.027	2.18 (0.87–5.41)	0.095
	< 24	1		1	
ER	Positive	0.91 (0.36–2.28)	0.837		
	Negative	1			
PR	Positive	1.08 (0.44–2.63)	0.875		
	Negative	1			
Her2/Neu	Positive	0.82 (0.34–2.02)	0.669		
	Negative	1			
Chemotherapy	No	3.09 (0.39–24.3)	0.284		
	Yes	1			
Radiotherapy	No	1.22 (0.49–3.04)	0.667		
	Yes	1			
FH	High	6.54 (1.85–23.16)	0.004	7.27 (2.04–25.95)	0.002
	Low	1		1	

\*Variables with  $p < 0.1$  were included in multivariable analysis

HR Hazard ratio, CI Confidence interval,—not applicable

capabilities and ROS levels in FH-OE cells were reduced following antimycin treatment (Fig. 4B & C). We also examined the effects of inhibiting electron transport on cell proliferation and migration, finding that treatment with Mitox20 peptide, an electron transport chain inhibitor [35], led to decreased proliferation and migration in MDA-MB-231 cells (Fig. 4D & E).

#### MMP1 downregulation and p21 Upregulation in FH knockdown breast cancer cells

To identify signaling pathways influenced by fumarate hydratase in breast cancer cells, we utilized next-generation sequencing (NGS) to compare differentially expressed genes in vector control and FH-knockdown cells. Analysis revealed that four genes—THBS1, MMP1, LCP1, and P3H2—were differentially expressed between control and knockdown cells (Supplementary Fig. S4 A). Western blot analysis confirmed that only MMP1 protein levels were significantly reduced, consistent with the RNA sequencing results (Supplementary Fig. S4 A & B). Ingenuity pathway analysis (IPA) indicated that MMP1 is connected to FH through p-ERK and p21 signaling (Supplementary Fig. S4 C). Our findings revealed that p21 was

upregulated while p-ERK and MMP1 were downregulated in breast cancer cells with FH knockdown, as determined by Western blot analysis (Fig. 5A). Conversely, FH-overexpressing cells demonstrated downregulation of p21 and upregulation of p-ERK and MMP1 (Fig. 5B). Notably, endogenous p21 expression in MDA-MB-231 cells is quite low compared to MCF-7 cells, and therefore lead to a mild increase of p21 expression when FH is downregulated, and a mild decrease of p21 expression when FH is upregulated, in MDA-MB-231 cells (Fig. 5).

Inhibiting p21 using UC2288 in FH knockdown cells resulted in increased MMP1 and p-ERK protein expression (Fig. 5C), suggesting that p21 is an upstream regulator of MMP1 and p-ERK. Additionally, treatment of FH-overexpressing cells with the MMP1 inhibitor GM6001 and the ERK phosphorylation inhibitor PD98059 indicated that MMP1 inhibition downregulated p-ERK expression, while inhibition of p-ERK did not affect MMP1 levels (Fig. 5D; Supplementary Fig. S4D), indicating that MMP1 is upstream of p-ERK. Furthermore, treatment with NAC and ascorbic acid increased p21 expression in FH-overexpressing MDA-MB-231 cells, suggesting a ROS-mediated regulation of

**Table 3** Univariate and multivariable analysis of overall survival for breast cancer patients

Variables	Categories	Univariate		Multivariable	
		HR (95%CI)	p-Value	HR (95%CI)	p-Value
Age (y)	>50	2.51 (0.67–9.47)	0.175		
	≤50	1			
Grade	III	2.46 (0.75–8.07)	0.137		
	I/II	1			
T status	T2-T4	1.31 (0.36–4.66)	0.677		
	T1	1			
N status	N1-3	1.08 (0.32–3.58)	0.905		
	N0	1			
BMI (kg/m <sup>2</sup> )	≥24	2.00 (0.61–6.58)	0.254		
	< 24	1			
ER	Positive	1.44 (0.38–5.45)	0.59		
	Negative	1			
PR	Positive	1.32 (0.39–4.54)	0.657		
	Negative	1			
Her2/Neu	Positive	3.36 (0.89–12.70)	0.075	4.09 (1.05–15.96)	0.043
	Negative	1		1	
Chemotherapy	No	1.84 (0.22–15.51)	0.577		
	Yes	1			
Radiotherapy	No	1.00 (0.30–3.38)	0.991		
	Yes	1			
FH	High	4.85 (1.02–23.12)	0.048	6.11 (1.17–31.98)	0.032
	Low	1		1	

\* Variables with  $p < 0.1$  were included in multivariable analysis

HR Hazard ratio, CI Confidence interval, —not applicable

p21 (Fig. 5E). Correlation analysis of FH with p-ERK and MMP1 in clinical tissue samples demonstrated a positive relationship between FH, p-ERK, and MMP1 but a negative correlation with p21 (Fig. 5F; Supplementary Fig. S4E).

#### FH knockdown in mouse breast cancer 4T1 cells reduces proliferation and invasion *In Vitro* and *In Vivo*

To explore the biological functions of FH *in vivo*, we performed FH knockdown in 4T1 mouse breast cancer cells using four distinct shRNAs, with shRNA clones 3 and 4 exhibiting superior knockdown efficiency (Fig. 6A). Similar to findings in human breast cancer cells, the knockdown of FH resulted in decreased cell proliferation and invasion in the 4T1 model (Fig. 6B & C). Additionally, we overexpressed both wild-type FH and its enzymatic mutant FH H235 N in 4T1 KD4 cells to assess whether the enzymatic activity of FH is crucial for its role in cell proliferation and migration (Fig. 6D). Restoration of proliferation and migration in FH-knockdown 4T1 cells was achieved following transfection with either wild-type FH or the catalytic-inactive FH H235 N mutant (Fig. 6E & F) [36].

To investigate the effect of fumarate hydratase (FH) on breast tumor growth, we employed a syngeneic mouse model using BALB/c mice and 4T1 mouse breast cancer cells. Our observations indicated that orthotopic mammary tumor growth was significantly reduced in 4T1 cells with FH knockdown, as measured by tumor volume and bioluminescent signals obtained from the IVIS imaging system (Fig. 7A & B). At the time of sacrifice, both tumor volume and weight were markedly lower in the FH knockdown group compared to the luciferase control (Luc control) group (Fig. 7C).

Additionally, we assessed the expression levels of FH, p21, and phosphorylated ERK (p-ERK) through immunohistochemistry (IHC) analysis. The results revealed decreased levels of both FH and p-ERK, along with increased p21 expression in FH-knockdown tumors when compared to the Luc control tumors (Fig. 7D). Weekly measurements of the mice's body weight and tumor images taken at the time of sacrifice are presented in Supplementary Fig. S5 A & B.

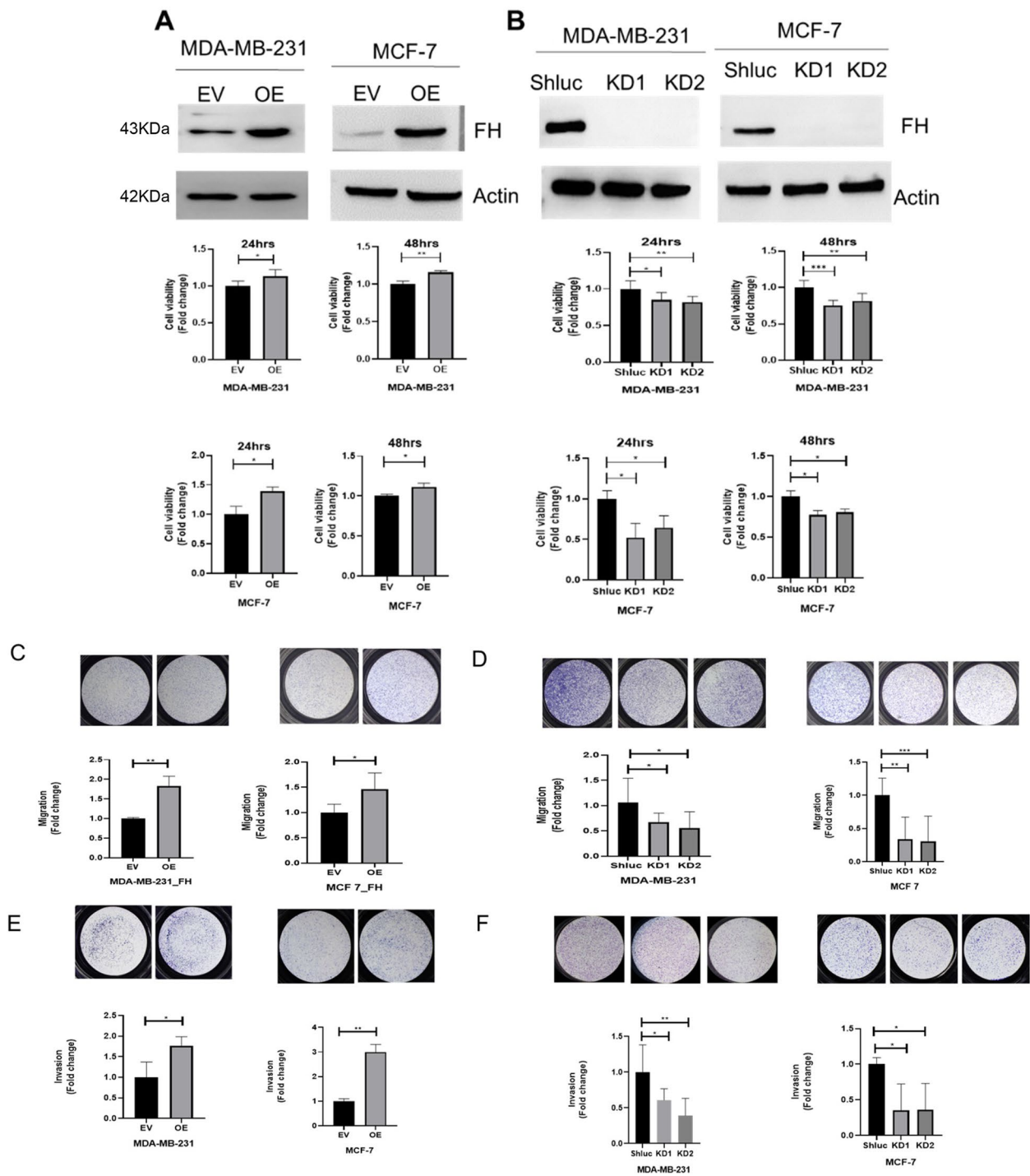


**Fig. 2** FH knockdown reduced breast cancer cell proliferation, migration and invasion abilities. **A** Cell proliferation in MDA-MB-231 (left) and MCF-7 (right) cells infected with empty vector control (EV) or FH-overexpressing (OE) lentivirus. **B** Cell proliferation in MDA-MB-231 (left) and MCF-7 (right) cells infected with shluc or FH shRNAs. **C** Cell migration ability of MDA-MB-231 and MCF-7 cells infected with vector controls, FH, shluc or FH shRNAs. **D** Cell invasion ability of MDA-MB-231 and MCF-7 cells infected with vector controls, FH, shluc or FH shRNAs. Proliferation assay was performed for 24 h and 48 h. Migration and invasion assays were performed for 24 h. The data shown represent the average of three independent repeats. Data are presented as mean  $\pm$  SD; \* $p$  < 0.05, \*\* $p$  < 0.01, \*\*\* $p$  < 0.001

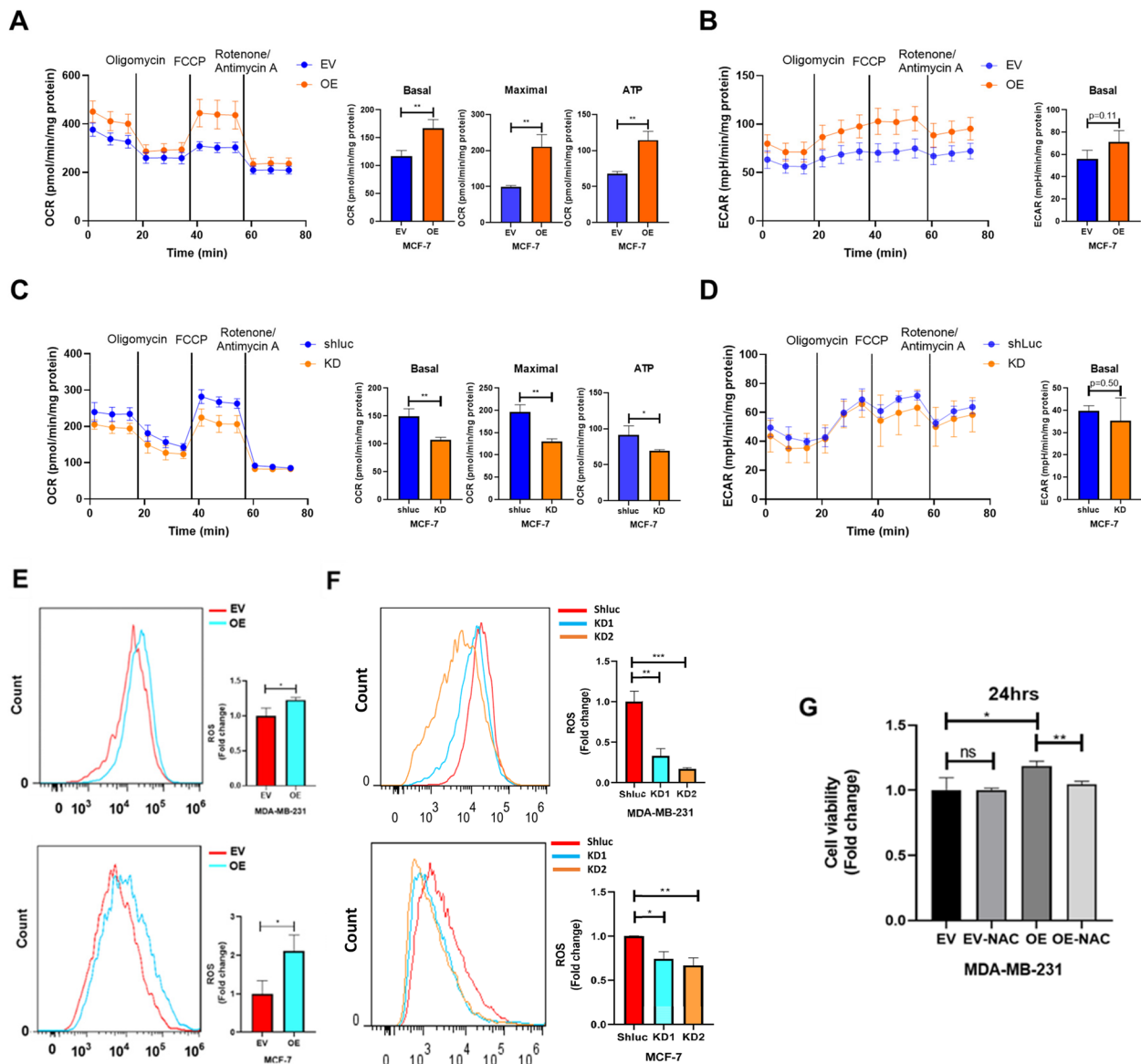


**Fig. 3** Extracellular acidification rate (ECAR) and oxygen consumption rate (OCR) were upregulated in FH-overexpressing (OE) breast cancer cells. **A & B** OCR and ECAR in FH-overexpressing MCF-7 cells. **C & D** OCR and ECAR in FH knockdown MCF-7 cells. **E** ROS level in FH-overexpressing MDA-MB-231 & MCF-7 cells. **F** ROS level in FH knockdown MDA-MB-231 & MCF-7 cells. **G** Effect of NAC (2 mM) on cell viability in FH-overexpressing MDA-MB-231 cells. The data shown represent the average of three independent repeats. Data are presented as mean  $\pm$  SD; \* $p < 0.05$  and \*\* $p < 0.01$ , \*\*\* $p < 0.001$

## Discussion

Our study provides evidence that fumarate hydratase (FH) plays a significant role in breast cancer progression, highlighting its potential as a prognostic biomarker and therapeutic target. While the role of FH as a tumor suppressor has been reported in uterine leiomyomas, soft tissue sarcoma, and renal cell carcinomas [19, 22, 23], the data presented here identifies novel and previously underexplored role for FH as an oncoprotein in breast cancer, exerting its effects through both metabolic and

non-metabolic pathways. A graphic abstract in Fig. 8 provides a summary for our findings on FH's role in breast cancer.

### FH promotes breast cancer cell proliferation and metastasis in a catalysis-independent manner

TCA cycle enzymes including FH provide precursors for the synthesis of other biomolecules for fueling cell growth and proliferation [37], and database analysis of human mitochondrial transcriptome from breast cancer

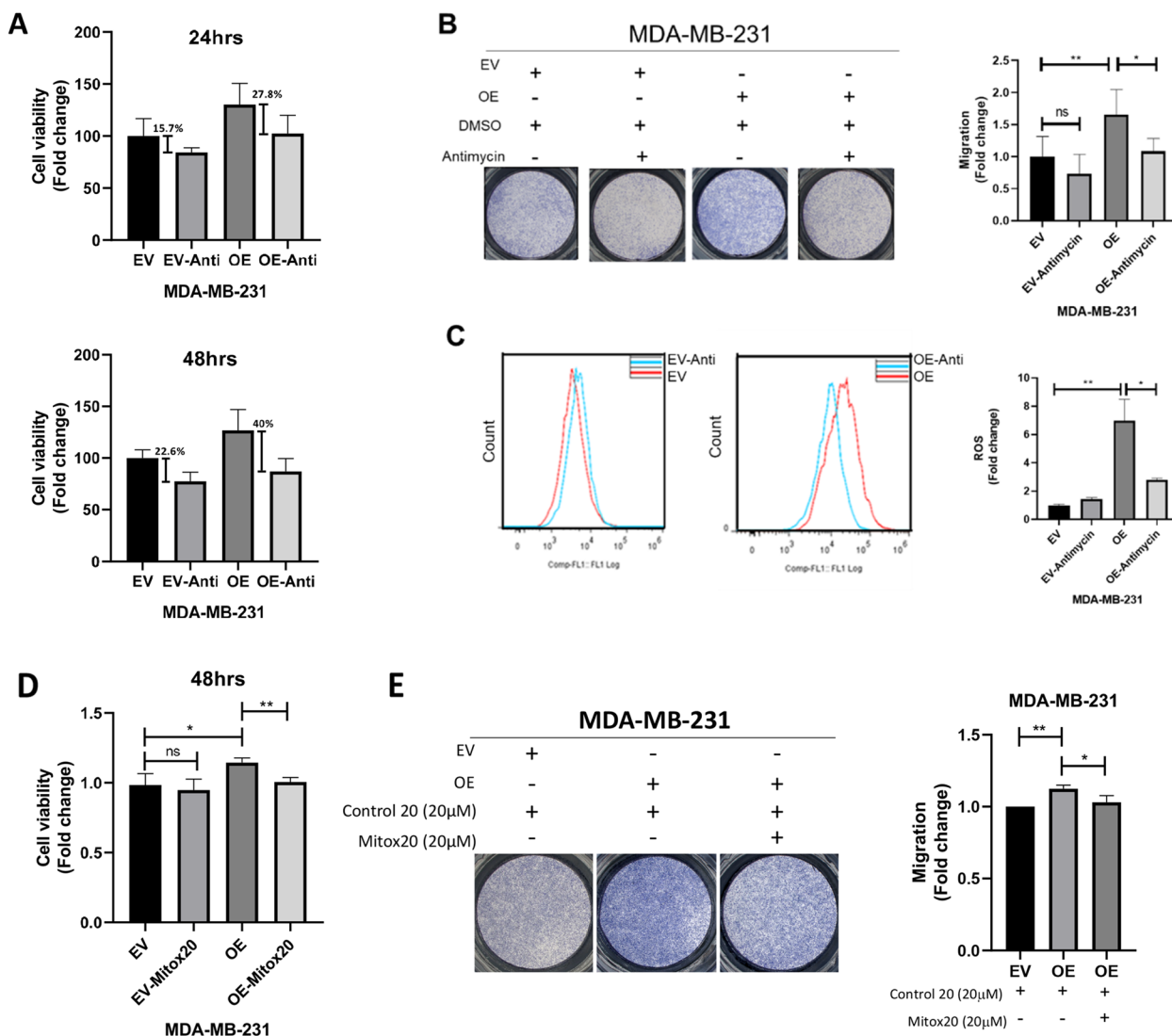


**Fig. 4** Antimycin treatment reduced cell proliferation in FH-overexpressing MDA-MB-231 breast cancer cells. **A** Cell viability of FH-overexpressed MDA-MB-231 cells after antimycin (0.5 µM) treatment for 24 h and 48 h. **B** Cell migration ability after antimycin treatment (0.5 µM, 24 h). **C** ROS level in FH-overexpressed MDA-MB-231 cells after antimycin treatment. **D** Cell viability of FH-overexpressed MDA-MB-231 cells after Mitox20 (20 µM) treatment for 48 h. **E** Cell migration of FH-overexpressed MDA-MB-231 cells after Mitox20 (20 µM) treatment for 24 h. The data shown represent the average of three independent repeats. Data are presented as mean ± SD; \**p* < 0.05, \*\**p* < 0.01, and \*\*\**p* < 0.001

cells suggests that FH is upregulated in breast cancer cells [38]. It is possible that FH-promoted breast cancer cell proliferation and migration/invasion may be in part mediated by upregulated biomolecule production. This has been observed with citrate synthase (CS), another TCA cycle enzyme, which is upregulated in prostate cancer and associated with decreased survival [39], and increases cell proliferation, migration, invasion and mitochondrial respiration [39].

While FH downregulation leads to a more evident decrease in cell viability (Fig. 2B), FH overexpression has a limited but significant increase in breast cancer cell viability

(Fig. 2A). One possible explanation for these results could be that overexpressed protein levels are above the threshold and lead to limited effect. Our study additionally suggested that catalytic activity may not be required for oncogenesis of FH, since FH H235 N mutant, with loss of catalytic activity, did not suppress FH-mediated breast cancer cell proliferation and migration (Fig. 6E&F).

#### FH activates mitochondrial metabolism and ROS generation to enhance breast cancer proliferation

Glycolysis generates not only energy but also organic molecules to build biomass and maintain cell growth

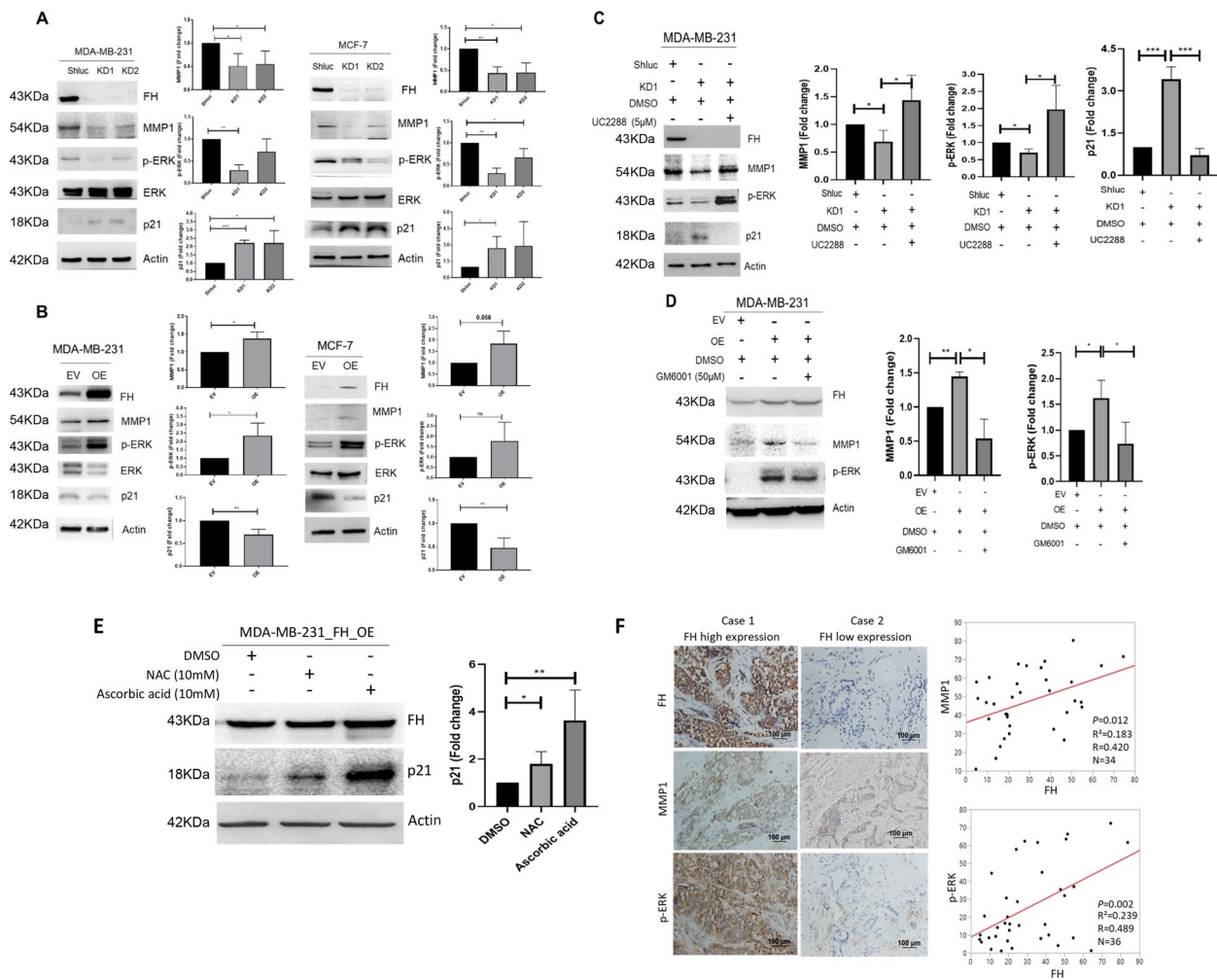


**Fig. 5** MMP1 expression was downregulated and p21 expression upregulated in FH knockdown cells. **A & B** MMP1, p-ERK, and p21 expression in FH knockdown and overexpressing MDA-MB-231 and MCF-7 cells and their quantification figures. **C** MMP1, p-ERK and p21 protein expression in p21 inhibitor UC2288 (5 μM, 48 h) treated FH knockdown MDA-MB-231 cells and their quantification. **D** MMP1 and p-ERK expression in MMP1 inhibitor GM6001 (50 μM, 6 h) treated FH overexpressed MDA-MB-231 cells and their quantification figure. **E** p21 expression in FH overexpressed MDA-MB-231 cells treated with ROS scavenger NAC (10 mM) or ascorbic acid (10 mM) for 24 h. **F** Left, FH, MMP1 and p-ERK protein expression in clinical samples evaluated by IHC; right, correlation of FH with MMP1 and p-ERK in clinical samples. The data shown represent the average of three independent repeats. Data are presented as mean ± SD; \**p* < 0.05, \*\**p* < 0.01, and \*\*\**p* < 0.001

[40], while mitochondrial metabolism produces ATP to support cell functions. In this study, both OCR—a measurement for mitochondrial metabolism and ECAR—a measurement for glycolysis, were upregulated by FH, a result similarly seen in ovarian cancer cells [40, 41]. Our results, suggesting that FH promotes OCR to support the proliferation of breast cancer cells, align with a previous report suggesting that cancer cells require increased biosynthesis of nucleotides, lipids, and proteins. This elevated demand leads to upregulated metabolic activity, which may in turn contribute to increased OCR [42]. Furthermore, it is well documented that ROS, byproducts of the respiration process in mitochondrial complexes I

and III, influences cancer cell behavior [43]. In agreement with this, we observed that FH enhanced ROS generation followed by elevated cell proliferation (Fig. 3E-G).

**FH activates MMP1 expression and inactivates p21 expression to promote malignant breast cancer behaviors**

Using next generation RNA sequencing, we discovered that matrix metalloproteinase 1 (MMP1) expression was activated by FH. MMP-1 is a zinc-dependent endopeptidase that cleaves the extracellular matrix [44], and is highly expressed in a variety of cancers including nasopharynx, lung, esophagus, and oral cavity [45–48]. It participates in different signaling pathways that promote

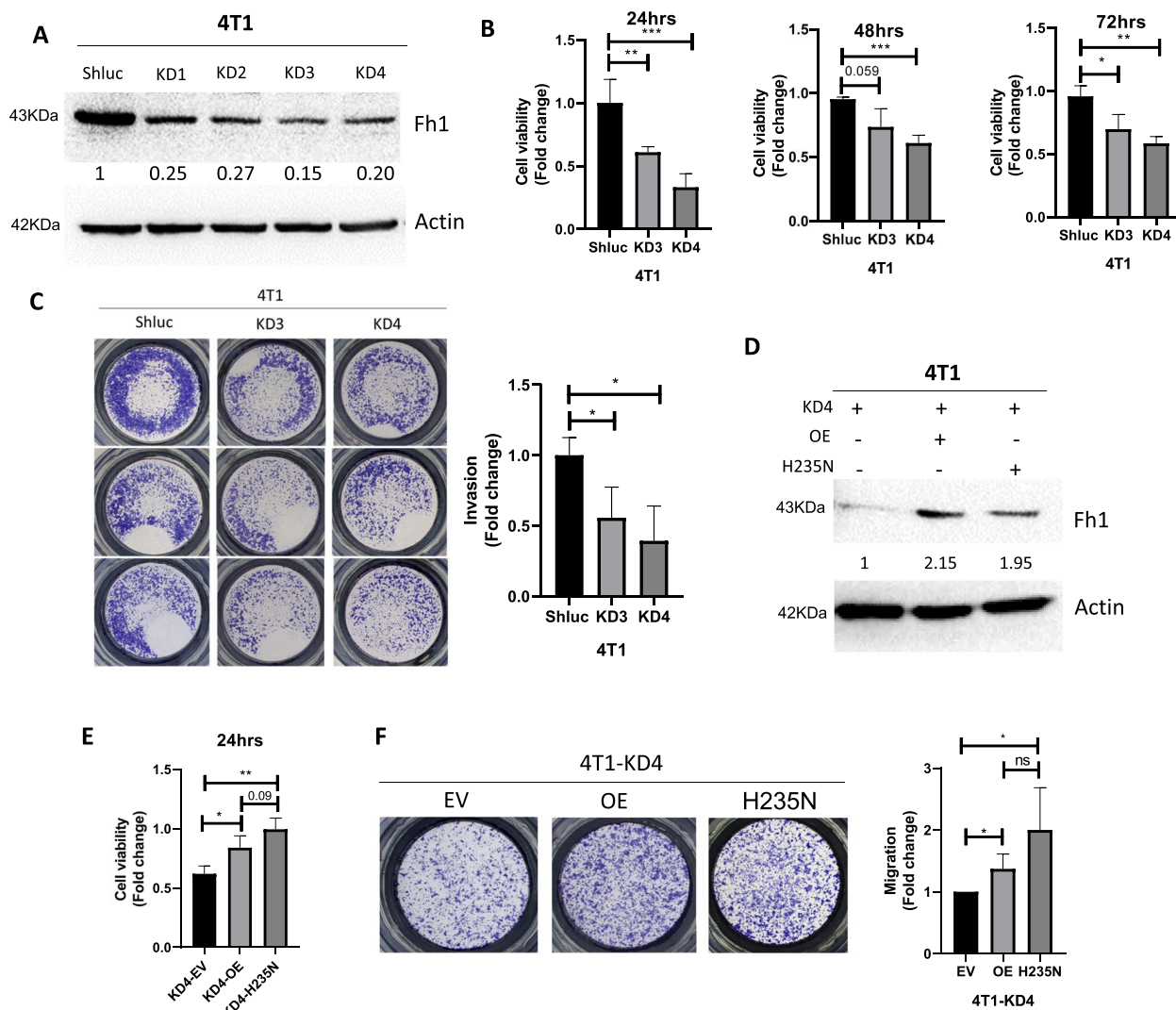


**Fig. 6** FH knockdown in mouse breast cancer 4T1 cells downregulated their proliferation and invasion abilities. **A** Western blot showing knockdown efficiency of four different clones targeting mouse Fh1 in 4T1 cell line. **B** Cell viability of FH knockdown 4T1 cells compared to control group. **C** Invasion ability of FH knockdown 4T1 cells compared to control group. **D** Western blot showing FH protein level in FH knockdown 4T1 (KD4 clone) cells after transfection with wild type FH or FH H235 N mutant. **E** Cell viability of FH knockdown 4T1 (KD4 clone) cells after transfection with wild type FH or FH H235 N mutant; right, bar graph showing quantification of migration results. The data shown represent the average of three independent repeats. Data are presented as mean  $\pm$  SD; \* $p$  < 0.05, \*\* $p$  < 0.01, and \*\*\* $p$  < 0.001

esophageal cancer cell proliferation and migration via activation of the PI3 K/AKT pathway [49] or downregulation of miR-188-5p to activate SOX2 and CDK4 [50]. MMP1 promotes drug resistance in lung cancer cells through fibroblast senescence [51, 52] and inhibition of p21, a cell cycle regulator that functions as a mediator of p53 in suppressing cell growth and promoting apoptosis [53], promotes MMP1 activation [54] and cancer cell proliferation and migration [55–57]. In breast cancer, MMP1 is a poor prognostic marker [58] and is involved in drug resistance [59, 60]. In agreement with these reports, we

observed that MMP1 is a downstream effector of p21 and its expression is activated by FH via p21 downregulation. Recent studies also revealed that elevated MMP1 levels in breast cancer-associated fibroblasts (CAFs) contribute to tumor advancement and poor prognosis [61]. p21 acts as a negative regulator of epithelial mesenchymal transition (EMT) by interaction with various genes [62, 63]. ERK is a prominent protein that plays a crucial role in several biological functions such as cell growth, movement, and invasion of cancer cells [64]. In our present study, we observed that ERK phosphorylation was

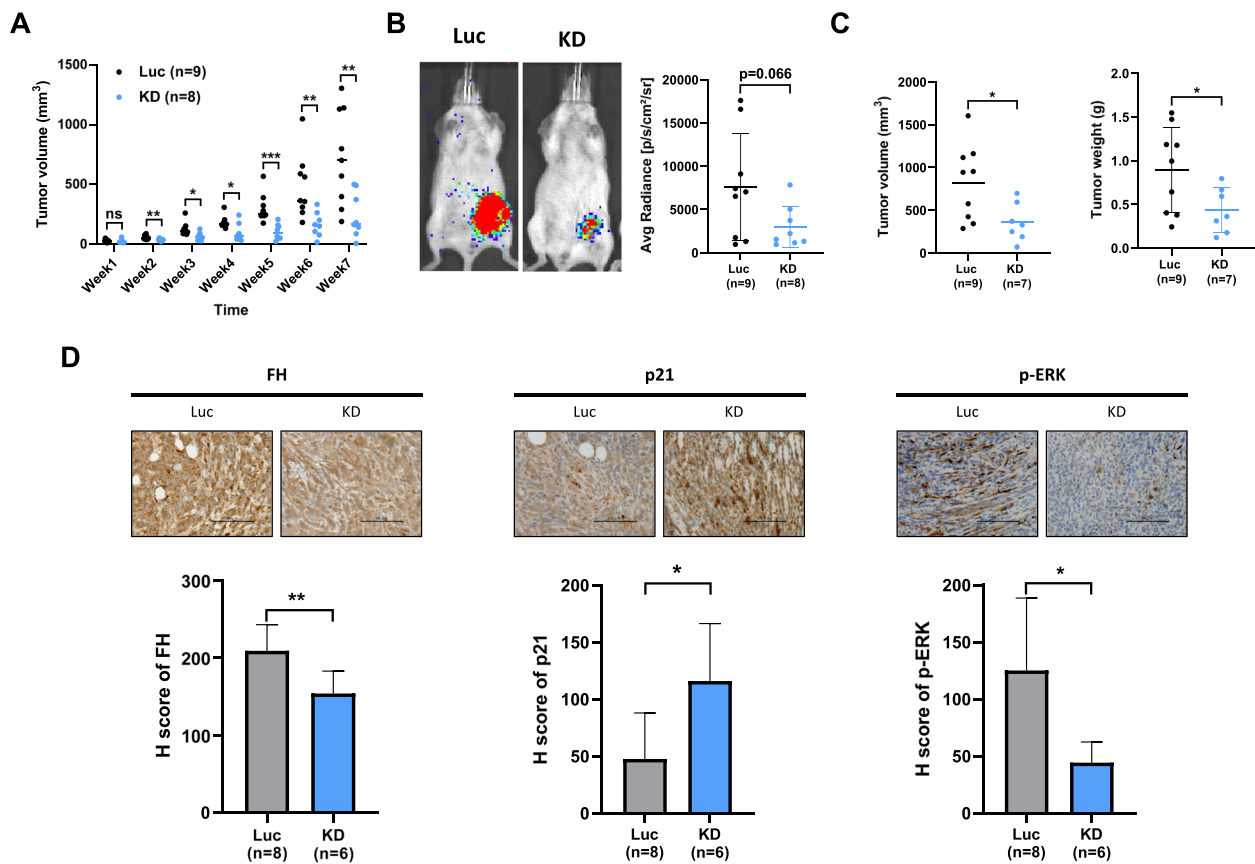


**Fig. 7** FH downregulation suppressed orthotopic breast tumor growth in mice. **A** Weekly measurement of tumor volume in control (Luc) group and FH knockdown (KD) group. **B** Bioluminescence level, as determined by IVIS, in the orthotopic tumors in FH knockdown (KD) group and control (Luc) group before sacrifice. **C** Tumor volume and tumor weight in FH knockdown (KD) group and control (Luc) group at sacrifice. **D** Expression of FH, p21 and p-ERK, as determined by IHC, in the orthotopic tumors of FH knockdown (KD) group and control (Luc) group. Of note, one mouse in the KD group died before sacrifice and was not included in Fig. 7 C result

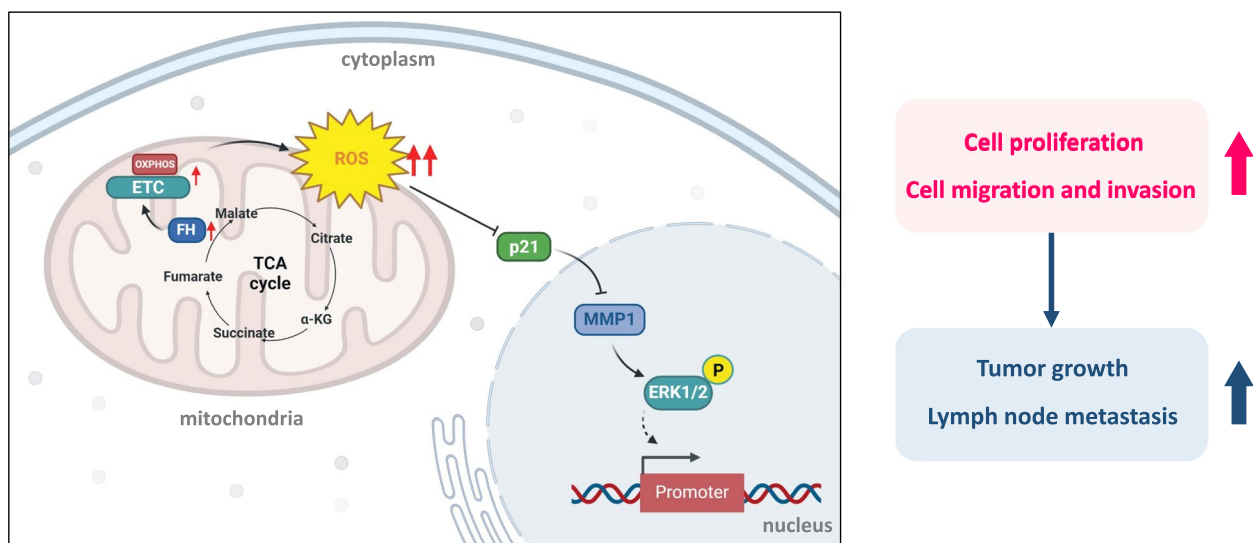


**Fig. 8** Schematic diagram showing FH signaling pathway in breast cancer. FH promotes breast cancer cell proliferation through upregulation of OCR, which results in upregulated ROS production. ROS further inhibits p21, which leads to upregulated MMP1 and p-ERK protein expression, resulting in upregulated cell proliferation and migration ability of breast cancer cells. Therefore, tumor growth and metastasis are enhanced

increased in FH overexpressed cells and decreased in FH knockdown cells. Also, p-ERK has been reported to be associated with poor survival in breast cancer patients [65].

### FH exerts oncogenic or tumor-suppressing activity in different cancer type settings

Previous studies report that FH functions as a tumor suppressor in renal, lung and endometrial cancers [21–23]. In this study, we provide direct evidence that FH promotes breast cancer progression. While our study clearly demonstrated a direct oncogenic role of FH in breast cancer, a recent study on maelstrom spermatogenic transposon silencer (MAEL) [66] showed that MAEL facilitates metabolic reprogramming from oxidative phosphorylation to glycolysis and promotes breast cancer progression via autophagic degradation of citrate synthase and fumarate hydratase [67], suggesting an indirect tumor-suppressing activity of FH in breast cancer. These contradictory results may stem from alternative downstream pathways of MAEL, potential FH and CS interactions, and non-metabolic effects of FH and CS which were not examined in this study.

This study has some limitations and unsolved questions. First, established prognostic markers, such as tumor grade, nodal status, ER, HER2, and others, are not significantly prognostic in our analysis in univariate and multivariable analysis (Table 2). Similar findings have also been reported by other groups [68–70]. The possibility of insufficient case numbers cannot be ruled out. Second, we did not check the mitochondrial ROS to confirm that increased ROS in FH-overexpressing cells is produced by mitochondrial activity. Third, only XTT colorimetric assay was applied for studying the short-term cell proliferation effect of FH before proceeding with orthotopic mouse model. It may be more appropriate to explore the long-term in vitro activity of FH, e.g. crystal violet staining or other clonogenic assays, before animal study [71, 72]. While our study suggest that FH suppresses the expression of p21, a senescence marker, to promote breast cancer cell proliferation, the possible involvement of p53 in modulating p21 expression after FH downregulation (Fig. 5) was not pursued in this study [73, 74]. Therefore, further efforts are required to clarify the role of FH in breast cancer.

In conclusion, our findings suggest FH as an important modulator of breast cancer cell survival, proliferation, and metastatic behavior through metabolic and signaling pathways. Given its association with poor clinical outcomes, targeting FH or its downstream pathways could offer a potential therapeutic avenue for managing aggressive breast cancer, justifying further

investigation into its functional roles and possibilities for translational applications.

### Abbreviations

ATP	Adenosine triphosphate
CS	Citrate synthase
DFS	Disease-free survival
ECAR	Extracellular acidification rate
ETC	Electron transport chain
FH	Fumarate hydratase
HRLCC	Hereditary leiomyomatosis and renal cell cancer
IPA	Ingenuity pathway analysis
IVIS	In vivo imaging system
MAEL	Maelstrom spermatogenic transposon silencer
MCUL	Multiple cutaneous and uterine leiomyomas
NAC	N-Acetylcysteine
NGS	Next generation sequencing
NHEJ	Non-homologous end joining
OCR	Oxygen consumption rate
OS	Overall survival
PBS	Phosphate-buffered saline
PBDF	Polyvinylidene fluoride
ROS	Reactive Oxygen Species
TCA	The tricarboxylic acid

### Supplementary Information

The online version contains supplementary material available at <https://doi.org/10.1186/s40170-025-00397-z>.

Supplementary Material 1

### Acknowledgements

The authors thank the Center for Laboratory Animals in Kaohsiung Medical University for the animal care and Center for Research Resources and Development in Kaohsiung Medical University for providing the service of TissueFaxs microscopy system. We also thank Professor Yi-Chen Lee for helping in statistical analysis of clinical data.

### Authors' contributions

S.S.F.Y., A.V., H.D.H.N., P.Y.C., C.H.T., C.H.W., Y.C.C., Y.C.W., S.C.S.H., S.L., M.F.H., and Y.Y.W. conceived and designed the study. S.S.F.Y., A.V., H.D.H.N., P.Y.C., and Y.Y.W. performed the experiments. S.S.F.Y., C.H.T., and Y.Y.W. analyzed and interpreted the data. S.S.F.Y., A.V., and Y.Y.W. wrote the manuscript. S.C.S.H., and S.L. critically revised the manuscript. All authors reviewed and approved the final manuscript.

### Funding

This work was supported by grants from the National Science and Technology Council (NSTC112-2314-B-037-112-MY3, NSTC112-2314-B-037-120, NSTC113-2314-B-037-045, NSTC113-2314-B-037-037) and the Center for Intelligent Drug Systems and Smart Biodevices (IDS2B) from the Featured Areas Research Center Program within the framework of the Higher Education Sprout Project by the Ministry of Education, Taiwan. This work was also supported by grants from Kaohsiung Medical University Hospital (KMUH109-9R44, KMUH110-0R43, KMUH111-1R37, KMUH112-2R42, KMUH-DK(A)110001, KMUH-DK(A)112001, KMUH-DK(A)113001) and Kaohsiung Medical University (KMU-DK(A)111005, KMU-DK(A)112006, KMU-DK(A)113002, NYCUKMU-111-1002, NYCU-KMU-112-1005, KMU-TC112 A03-5, NYCUKMU-113-1002), Taiwan.

### Data availability

No datasets were generated or analysed during the current study.

### Declarations

#### Ethics approval and consent to participate

This study was approved by the institutional review board of Kaohsiung Medical University Hospital (KMUHIRB-F(I)-20180112, KMUHIRB-E(I)-20180136,

KMUHIRB-E(1)-20200299) and the Institutional Animal Care and Utilization Committee of Kaohsiung Medical University (IACUC number:109046).

#### Consent for publication

Not applicable.

#### Competing interests

The authors declare no competing interests.

#### Author details

<sup>1</sup>Graduate Institute of Medicine, College of Medicine, Kaohsiung Medical University, Kaohsiung, Taiwan. <sup>2</sup>Translational Research Center, Kaohsiung Medical University Hospital, Kaohsiung 807, Taiwan. <sup>3</sup>Department of Obstetrics and Gynecology, Kaohsiung Medical University Hospital, Kaohsiung 807, Taiwan. <sup>4</sup>Department of Medical Research, Kaohsiung Medical University Hospital, Kaohsiung 807, Taiwan. <sup>5</sup>Drug Development and Value Creation Research Center, Kaohsiung Medical University, Kaohsiung 807, Taiwan. <sup>6</sup>Department of Biological Science and Technology, Institute of Molecular Medicine and Bioengineering, Center for Intelligent Drug Systems and Smart Biodevices (IDS2B), National Yang Ming Chiao Tung University, 75 Bo-Ai Street, Hsinchu 300, Taiwan. <sup>7</sup>School of Dentistry, College of Dental Medicine, Kaohsiung Medical University, Kaohsiung 807, Taiwan. <sup>8</sup>Division of Oral Pathology & Maxillofacial Radiology, Kaohsiung Medical University Hospital, Kaohsiung 807, Taiwan. <sup>9</sup>School of Medicine, College of Medicine, Kaohsiung Medical University, Kaohsiung 807, Taiwan. <sup>10</sup>Division of Plastic Surgery, Department of Surgery, Kaohsiung Medical University Hospital, Kaohsiung 807, Taiwan. <sup>11</sup>Division of Breast Oncology and Surgery, Department of Surgery, Kaohsiung Medical University Hospital, Kaohsiung 807, Taiwan. <sup>12</sup>Department of Dermatology, College of Medicine, Kaohsiung Medical University, Kaohsiung 807, Taiwan. <sup>13</sup>Department of Dermatology, Kaohsiung Medical University Hospital, Kaohsiung 807, Taiwan. <sup>14</sup>Canniesburn Regional Plastic Surgery and Burns Unit, College of Medical, Veterinary and Life Sciences, University of Glasgow, Glasgow G4 0SFG12 8QQ, UK. <sup>15</sup>Department of Biomedical Science and Environmental Biology, College of Life Science, Kaohsiung Medical University, Kaohsiung 807, Taiwan. <sup>16</sup>National Center for Geriatrics and Welfare Research, National Health Research Institutes, No. 8, Xuefu W. RdYunlin County 632, Huwei Township, Taiwan.

Received: 4 January 2025 Accepted: 24 May 2025

Published online: 29 May 2025

#### References

- Bray F, Laversanne M, Sung H, Ferlay J, Siegel RL, Soerjomataram I, Jemal A, Global cancer statistics, GLOBOCAN estimates of incidence and mortality worldwide for 36 cancers in 185 countries. *CA Cancer J Clin*. 2022;74(2024):229–63.
- Hong R, Xu B. Breast cancer: an up-to-date review and future perspectives. *Cancer Commun (Lond)*. 2022;42:913–36.
- Liu Y, Zhou Q, Song S, Tang S. Integrating metabolic reprogramming and metabolic imaging to predict breast cancer therapeutic responses. *Trends Endocrinol Metab*. 2021;32:762–75.
- Dias AS, Almeida CR, Helguero LA, Duarte IF. Metabolic crosstalk in the breast cancer microenvironment. *Eur J Cancer*. 2019;121:154–71.
- Kroemer G, Pouyssegur J. Tumor cell metabolism: cancer's Achilles' heel. *Cancer Cell*. 2008;13:472–82.
- Xiao Y, Yu TJ, Xu Y, Ding R, Wang YP, Jiang YZ, Shao ZM. Emerging therapies in cancer metabolism. *Cell Metab*. 2023;35:1283–303.
- Warburg O, Posener K, Negelein E. Über den Stoffwechsel der Tumoren. *Biochemische Zeitschrift*. 1924;152:319–44.
- Sajjani K, Islam F, Smith RA, Gopalan V, Lam AK-Y. Genetic alterations in Krebs cycle and its impact on cancer pathogenesis. *Biochimie*. 2017;135:164–72.
- Wang Y, Patti GJ. The Warburg effect: a signature of mitochondrial overload. *Trends Cell Biol*. 2023;33:1014–20.
- Bedi M, Ray M, Ghosh A. Active mitochondrial respiration in cancer: a target for the drug. *Mol Cell Biochem*. 2022;477:345–61.
- Sreedhar A, Zhao Y. Dysregulated metabolic enzymes and metabolic reprogramming in cancer cells. *Biomedical reports*. 2018;8:3–10.
- I. Scheffler, *Mitochondria*, 2nd edn. J. Wiley and Sons, Inc., Hoboken, New Jersey, 2008.
- Anderson NM, Mucka P, Kern JG, Feng H. The emerging role and targetability of the TCA cycle in cancer metabolism. *Protein Cell*. 2018;9:216–37.
- Zong WX, Rabinowitz JD, White E. *Mitochondria and Cancer*. *Mol Cell*. 2016;61:667–76.
- Ryan DG, Murphy MP, Frezza C, Prag HA, Chouchani ET, O'Neill LA, Mills EL. Coupling Krebs cycle metabolites to signalling in immunity and cancer. *Nat Metab*. 2019;1:16–33.
- Gasmi A, Peana M, Arshad M, Butnariu M, Menzel A, Björklund G. Krebs cycle: activators, inhibitors and their roles in the modulation of carcinogenesis. *Arch Toxicol*. 2021;95:1161–78.
- Leshets M, Silas YB, Lehming N, Pines O. Fumarate: from the TCA Cycle to DNA damage response and tumor suppression. *Front Mol Biosci*. 2018;5:68.
- Valcarcel-Jimenez L, Frezza C. Fumarate hydratase (FH) and cancer: a paradigm of oncometabolism. *Br J Cancer*. 2023;129:1546–57.
- Schmidt C, Sciacovelli M, Frezza C. Fumarate hydratase in cancer: A multifaceted tumour suppressor. *Semin Cell Dev Biol*. 2020;98:15–25.
- Raimundo N, Baysal BE, Shadel GS. Revisiting the TCA cycle: signaling to tumor formation. *Trends Mol Med*. 2011;17:641–9.
- Linehan WM, Rouault TA. Molecular pathways: Fumarate hydratase-deficient kidney cancer—targeting the Warburg effect in cancer. *Clin Cancer Res*. 2013;19:3345–52.
- Wang YY, Vadhan A, Wu CH, Hsu CY, Chen YC, Chen YK, Chen PY, Nguyen HDH, Chang YC, Yuan SF. Fumarate hydratase functions as a tumor suppressor in endometrial cancer by inactivating EGFR signaling. *Oncol Rep*. 2023;50:183.
- Vadhan A, Yang YF, Wang YM, Chen PY, Tzou SC, Cheng KH, Hu SC, Cheng TL, Wang YY, Yuan SF. Fumarate hydratase inhibits non-small cell lung cancer metastasis via inactivation of AMPK and upregulation of DAB2. *Oncol Lett*. 2023;25:42.
- Kiuru M, Lehtonen R, Eerola H, Aittomäki K, Blomqvist C, Nevanlinna H, Aaltonen LA, Launonen V. No germline FH mutations in familial breast cancer patients. *Eur J Hum Genet*. 2005;13:506.
- Huang KT, Dobrovic A, Fox SB. No evidence for promoter region methylation of the succinate dehydrogenase and fumarate hydratase tumour suppressor genes in breast cancer. *BMC Res Notes*. 2009;2:194.
- Lei J, Pan Y, Gao R, He B, Wang Z, Lei X, Zhang Z, Yang N, Yan M. Ratacarpine induces the differentiation of triple-negative breast cancer cells through inhibiting fumarate hydratase. *J Transl Med*. 2023;21:553.
- Sang L, Ju HQ, Yang Z, Ge Q, Zhang Z, Liu F, Yang L, Gong H, Shi C, Qu L, Chen H, Wu M, Chen H, Li R, Zhuang Q, Piao H, Yan Q, Yu W, Wang L, Shao J, Liu J, Wang W, Zhou T, Lin A. Mitochondrial long non-coding RNA GAS5 tunes TCA metabolism in response to nutrient stress. *Nat Metab*. 2021;3:90–106.
- Yuan SF, Wang YM, Chan LP, Hung AC, Nguyen HDH, Chen YK, Hu SC, Lo S, Wang YY. IL-1RA promotes oral squamous cell carcinoma malignancy through mitochondrial metabolism-mediated EGFR/JNK/SOX2 pathway. *J Transl Med*. 2023;21:473.
- Wang YY, Chen YK, Lo S, Chi TC, Chen YH, Hu SC, Chen YW, Jiang SS, Tsai FY, Liu W, Li RN, Hsieh YC, Huang CJ, Yuan SF. MRE11 promotes oral cancer progression through RUNX2/CXCR4/AKT/FOXO2 signaling in a nuclease-independent manner. *Oncogene*. 2021;40:3510–32.
- Györfy B, Lanczky A, Eklund AC, Denkert C, Budczies J, Li Q, Szallasi Z. An online survival analysis tool to rapidly assess the effect of 22,277 genes on breast cancer prognosis using microarray data of 1,809 patients. *Breast Cancer Res Treat*. 2010;123:725–31.
- Chandrasekar DS, Bashel B, Balasubramanya SAH, Creighton CJ, Ponce-Rodriguez I, Chakravarthi B, Varambally S. UALCAN: a portal for facilitating tumor subgroup gene expression and survival analyses. *Neoplasia*. 2017;19:649–658.
- Uhlen M, Zhang C, Lee S, Sjöstedt E, Fagerberg L, Bidkhori G, Benfaisas R, Arif M, Liu Z, Edfors F, Sanli K, von Feilitzen K, Oksvold P, Lundberg E, Hober S, Nilsson P, Mattsson J, Schwenk JM, Brunnström H, Glimelius B, Sjöblom T, Edqvist PH, Djureinovic D, Micke P, Lindskog C, Mardinoglu A, Ponten F. A pathology atlas of the human cancer transcriptome. *Sci*. 2017;357:eaan2507.
- Daniel RR, Jianjun Y, Shanker K, Nandan D, Radhika V, Debashis G, Terrence B, Akhilesh P, Arul MC. ONCOMINE: a cancer microarray database and integrated data-mining platform. *Neoplasia*. 2004;6:1–6.

34. Okoye CN, Koren SA, Wojtovich AP. Mitochondrial complex I ROS production and redox signaling in hypoxia. *Redox Biol.* 2023;67: 102926.
35. Giddings EL, Champagne DP, Wu M-H, Laffin JM, Thornton TM, Valenca-Pereira F, Culp-Hill R, Fortner KA, Romero N, East J, Cao P, Arias-Pulido H, Sidhu KS, Silverstrim B, Kam Y, Kelley S, Pereira M, Bates SE, Bunn JY, Fiering SN, Matthews DE, Robey RW, Stich D, D'Alessandro A, Rincon M. Mitochondrial ATP fuels ABC transporter-mediated drug efflux in cancer chemoresistance. *Nat Commun.* 2021;12:2804.
36. Subasri S, Chaudhary SK, Sekar K, Keshnerwani M, Velmurugan D. Molecular docking and molecular dynamics simulations of fumarate hydratase and its mutant H235N complexed with pyromellitic acid and citrate. *J Bioinform Comput Biol.* 2017;15:1750026.
37. DeBerardinis RJ, Lum JJ, Hatzivassiliou G, Thompson CB. The biology of cancer: metabolic reprogramming fuels cell growth and proliferation. *Cell Metab.* 2008;7:11–20.
38. Zhang Q, Liang Z, Gao Y, Teng M, Niu L. Differentially expressed mitochondrial genes in breast cancer cells: Potential new targets for anti-cancer therapies. *Gene.* 2017;596:45–52.
39. Cai Z, Deng Y, Ye J, Zhuo Y, Liu Z, Liang Y, Zhang H, Zhu X, Luo Y, Feng Y. Aberrant expression of citrate synthase is linked to disease progression and clinical outcome in prostate cancer. *Cancer management and research.* 2020;12:6149.
40. M.G. Vander Heiden, L.C. Cantley, C.B. Thompson, Understanding the Warburg effect: the metabolic requirements of cell proliferation, *Science*, 324 (2009) 1029–1033.
41. Kaur P, Nagar S, Bhagwat M, Uddin M, Zhu Y, Vancurova J, Vancura A. Activated heme synthesis regulates glycolysis and oxidative metabolism in breast and ovarian cancer cells. *PLoS ONE.* 2021;16: e0260400.
42. DeBerardinis RJ, Chandel NS. Fundamentals of cancer metabolism. *Sci Adv.* 2016;2: e1600200.
43. Kuznetsov AV, Margreiter R, Ausserlechner MJ, Hagenbuchner J. The Complex Interplay between Mitochondria. ROS and Entire Cellular Metabolism, *Antioxidants.* 2022;11:1995.
44. Bassiouni W, Ali MAM, Schulz R. Multifunctional intracellular matrix metalloproteinases: implications in disease. *Febs j.* 2021;288:7162–82.
45. Gong D, Li Z, Ding R, Cheng M, Huang H, Liu A, Kang M, He H, Xu Y, Shao J, Wang Y, Duan C. Extensive serum biomarker analysis in patients with nasopharyngeal carcinoma. *Cytokine.* 2019;118:107–14.
46. Schütz A, Röser K, Klitzsch J, Lieder F, Aberger F, Gruber W, Mueller KM, Pupyshv A, Moriggl R, Friedrich K. Lung Adenocarcinomas and Lung Cancer Cell Lines Show Association of MMP-1 Expression With STAT3 Activation. *Transl Oncol.* 2015;8:97–105.
47. Murray GI, Duncan ME, O'Neil P, McKay JA, Melvin WT, Fothergill JE. Matrix metalloproteinase-1 is associated with poor prognosis in oesophageal cancer. *J Pathol.* 1998;185:256–61.
48. Miguel AFP, Mello FW, Melo G, Rivero ERC. Association between immunohistochemical expression of matrix metalloproteinases and metastasis in oral squamous cell carcinoma: Systematic review and meta-analysis. *Head Neck.* 2020;42:569–84.
49. Cabral-Pacheco GA, Garza-Veloz I, Castruita-De la Rosa C, Ramirez-Acuña JM, Perez-Romero BA, Guerrero-Rodriguez JF, Martinez-Avila N, Martinez-Fierro ML, The roles of matrix metalloproteinases and their inhibitors in human diseases. *Int J Mol Sci.* 2020;21:9739.
50. Wang C, Mao C, Lai Y, Cai Z, Chen W. MMP1 3' UTR facilitates the proliferation and migration of human oral squamous cell carcinoma by sponging miR-188-5p to up-regulate SOX4 and CDK4. *Mol Cell Biochem.* 2021;476:785–96.
51. Gabasa M, Radisky ES, Ikemori R, Bertolini G, Arshakyan M, Hockla A, Duch P, Rondonone O, Llorente A, Maqueda M. MMP1 drives tumor progression in large cell carcinoma of the lung through fibroblast senescence. *Cancer Lett.* 2021;507:1–12.
52. Zhou H, Xiang Q, Hu C, Zhang J, Zhang Q, Zhang R. Identification of MMP1 as a potential gene conferring erlotinib resistance in non-small cell lung cancer based on bioinformatics analyses. *Hereditas.* 2020;157:32.
53. Engeland K. Cell cycle regulation: p53–p21-RB signaling. *Cell Death Differ.* 2022;29:946–60.
54. Perlman H, Bradley K, Liu H, Cole S, Shamiyeh E, Smith RC, Walsh K, Fiore S, Koch AE, Firestein GS. IL-6 and matrix metalloproteinase-1 are regulated by the cyclin-dependent kinase inhibitor p21 in synovial fibroblasts. *J Immunol.* 2003;170:838–45.
55. Bahl R, Arora S, Nath N, Mathur M, Shukla NK, Ralhan R. Novel polymorphism in p21waf1/cip1 cyclin dependent kinase inhibitor gene: association with human esophageal cancer. *Oncogene.* 2000;19:323–8.
56. Abbas T, Dutta A. p21 in cancer: intricate networks and multiple activities. *Nat Rev Cancer.* 2009;9:400–14.
57. Li Z, Qiu R, Qiu X, Tian T. SNHG6 promotes tumor growth via repression of P21 in colorectal cancer. *Cell Physiol Biochem.* 2018;49:463–78.
58. Wang J, Ye C, Lu D, Chen Y, Jia Y, Ying X, Xiong H, Zhao W, Zhou J, Wang L. Matrix metalloproteinase-1 expression in breast carcinoma: a marker for unfavorable prognosis. *Oncotarget.* 2017;8:91379–90.
59. Shen CJ, Kuo YL, Chen CC, Chen MJ, Cheng YM. MMP1 expression is activated by Slug and enhances multi-drug resistance (MDR) in breast cancer. *PLoS ONE.* 2017;12: e0174487.
60. Kim HW, Park JE, Baek M, Kim H, Ji HW, Yun SH, Jeong D, Ham J, Park S, Lu X, Kang HS, Kim SJ. Matrix metalloproteinase-1 (MMP1) upregulation through promoter hypomethylation enhances tamoxifen resistance in breast cancer. *Cancers (Basel).* 2022;14:1232.
61. Xi C, Song Z, Cui Q, Zhao Y, Li K, Kang H. Elevated MMP1 Expression in Carcinoma-Associated Fibroblasts of Breast Cancer Contributes to Tumor Progression and Unfavorable Prognosis. *Ann Clin Lab Sci.* 2024;54:66–75.
62. Liu M, Casimiro MC, Wang C, Shirley LA, Jiao X, Katiyar S, Ju X, Li Z, Yu Z, Zhou J. p21CIP1 attenuates Ras-and c-Myc-dependent breast tumor epithelial mesenchymal transition and cancer stem cell-like gene expression in vivo. *Proc Natl Acad Sci.* 2009;106:19035–9.
63. Zhang Y, Yan W, Jung YS, Chen X. PUMA cooperates with p21 to regulate mammary epithelial morphogenesis and epithelial-to-mesenchymal transition. *PLoS ONE.* 2013;8: e66464.
64. Wang YY, Vadhan A, Chen PH, Lee YL, Chao CY, Cheng KH, Chang YC, Hu SC, Yuan SF. CD44 promotes lung cancer cell metastasis through ERK-ZEB1 Signaling. *Cancers (Basel).* 2021;13:4057.
65. Bartholomeusz C, Gonzalez-Angulo AM, Liu P, Hayashi N, Lluch A, Ferrer-Lozano J, Hortobágyi GN. High ERK protein expression levels correlate with shorter survival in triple-negative breast cancer patients. *Oncologist.* 2012;17:766–74.
66. Sato K, Siomi MC. Functional and structural insights into the piRNA factor Maelstrom. *FEBS Lett.* 2015;589:1688–93.
67. Zhou L, Ou S, Liang T, Li M, Xiao P, Cheng J, Zhou J, Yuan L. MAEL facilitates metabolic reprogramming and breast cancer progression by promoting the degradation of citrate synthase and fumarate hydratase via chaperone-mediated autophagy. *Febs j.* 2023;290:3614–28.
68. Hida AI, Sagara Y, Yotsumoto D, Kanemitsu S, Kawano J, Baba S, Rai Y, Oshiro Y, Aogi K, Sagara Y, Ohi Y. Prognostic and predictive impacts of tumor-infiltrating lymphocytes differ between Triple-negative and HER2-positive breast cancers treated with standard systemic therapies. *Breast Cancer Res Treat.* 2016;158:1–9.
69. Yang SX, Polley EC. Systemic treatment and radiotherapy, breast cancer subtypes, and survival after long-term clinical follow-up. *Breast Cancer Res Treat.* 2019;175:287–95.
70. Vadhan A, Wang YY, Yuan SF, Lee YC, Hu SC, Huang JY, Ishikawa T, Hou MF. EMI2 expression as a poor prognostic factor in patients with breast cancer. *Kaohsiung J Med Sci.* 2020;36:640–8.
71. Vega-Avila E, Pugsley MK. An overview of colorimetric assay methods used to assess survival or proliferation of mammalian cells. *Proc West Pharmacol Soc.* 2011;54:10–4.
72. Brix N, Samaga D, Belka C, Zitzelsberger H, Lauber K. Analysis of clonogenic growth in vitro. *Nat Protoc.* 2021;16:4963–91.
73. Manousakis E, Miralles CM, Esquerda MG, Wright RHG. CDKN1A/p21 in Breast cancer: part of the problem, or part of the solution?. *Int J Mol Sci.* 2023;24:17488.
74. Yan J, Chen S, Yi Z, Zhao R, Zhu J, Ding S, Wu J. The role of p21 in cellular senescence and aging-related diseases. *Mol Cells.* 2024;47: 100113.

## Publisher's Note

Springer Nature remains neutral with regard to jurisdictional claims in published maps and institutional affiliations.